PHOTO COURTESY OF NY WATERWAY

By Jesus M. De la Cruz, Joaquín Aranda, Jose M. Giron-Sierra, Francisco Velasco, Segundo Esteban, Jose M. Diaz, and Bonifacio de Andres-Toro

New developments in naval architecture focus on fast ships for passenger and freight transportation. During 1970–1990 most new passenger ferries were built with speeds in the range 35–40 kn and were considered to be fast. Since 1990, the speed of new fast ferries has increased, reaching 70 kn. The ferry market is growing, with currently more than 200 companies handling 1,250 fast ferries. In Europe, 82.6 million passengers and 12.8 million cars were transported on fast ships in 2000. Fast freight ships are beginning to be considered. For example, several container vessels now under construction will be able to cross the Atlantic between North America and Europe in less than four days with speeds of up to 40 kn. New technologies are being developed to achieve the necessary performance and make fast ships competitive with other transportation alternatives, including aluminium hulls, propulsion systems, and ship designs [1].

Waves induce vertical accelerations on the ship, potentially causing seasickness, a major drawback for passengers. In addition, excessive vertical motions of the ship can be dangerous, causing slamming, or

0272-1708/04/$20.00©2004IEEE

deck wetness. There are several ways to smooth vertical motion. One approach is to use active appendages to counteract incident waves. The problem for automatic control is to maximize the efficiency of the appendages.

This article follows the chronological development of our research. First, we consider the main aspects of the problem to be solved, namely, seasickness, sea states, and ship motions.

Our research comprises two main steps: to develop a tool for control design in the form of a computer-based simulation and to use this tool to develop satisfactory controllers.

Although research on antipitching appendages started 40 years ago [2]–[5], few papers have considered the issue [6]–[8]. With the recent increase in fast ferries, moving appendages have been introduced, and the problem of ride control has reemerged [9]–[15].

Our research focuses on navigating a ship in head seas. For the ship we consider, two flaps at the transom and a T-foil near the bow are the moving actuators. The research comprises two main steps: first, to develop a tool for control design in the form of a computer-based simulation, and second, to use this tool to develop satisfactory controllers. The simulation is based on mathematical models of the ship, the actuators, the waves, and the seasickness effect. Extensive experimental work has been performed to construct a model of the ship's vertical motions. Experiments were also performed to validate improvements resulting from active control.

Seasickness, Sea States, and Ship Motions

Studies on seasickness published in 1974 [16] conclude that seasickness is a cumulative effect related to vertical acceleration at certain frequencies. There is a frequency band around 1 rad/s [Figure 1(a)], which is most effective for inducing seasickness. In these studies, a mathematical model of motion sickness incidence (MSI), an index defined as the percentage of subjects who became ill after two hours of motion, is given by

$$\mathrm{MSI} = 100 \cdot \left[0.5 \pm \mathrm{erf}\left(\frac{\pm \log_{10}(|a_v|/g) \mp \mu_{\mathrm{MSI}}}{0.4} \right) \right], \qquad (1)$$

where erf is the error function; $|a_v|$ is the vertical acceleration, averaged over a half-motion cycle, in a chosen place; and μ_{MSI} is given by the empirical expression

$$\mu_{\mathrm{MSI}} = -0.819 + 2.32(\log_{10} \omega_e)^2,$$

where ω_e is the dominant frequency (rad/s) of the vertical acceleration.

Ocean waves are generated by wind, and constant-direction wind over great distances can generate large waves. By statistical means, a description of ocean waves can be given in terms of wave energy spectra [17]. The World Meteorological Organization (WMO) distinguishes ten sea states [17] whose characteristics are listed in Table 1. According to [17] the significant wave height, in Table 1, is the mean value of the highest third of many measurements of wave amplitude. The "highest third" is defined as follows: supposing that there are N measurements of wave amplitude, they are arranged in order of magnitude from the highest to the lowest, and then the highest $N/3$ mea-

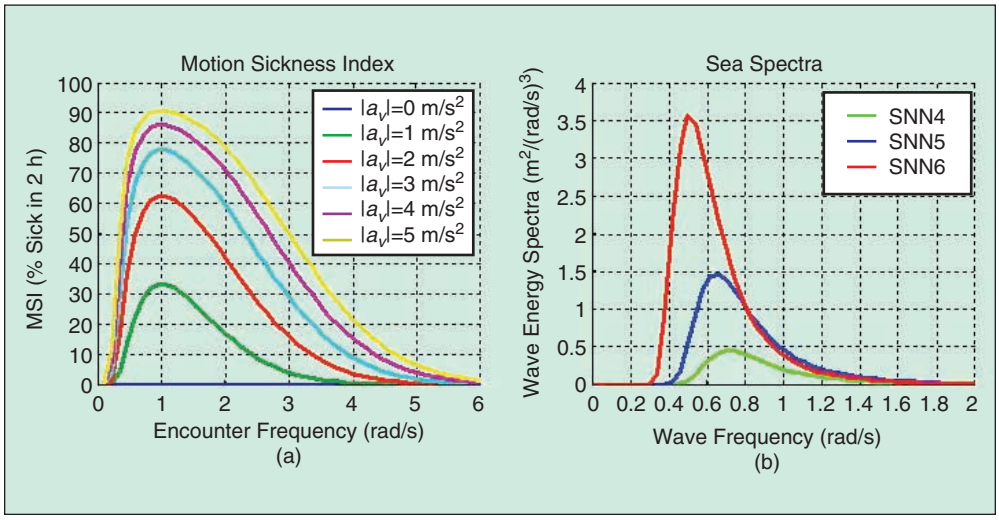

Figure 1. *Characteristics of the excitation and its effects: (a) seasickness is caused by oscillatory vertical accelerations with frequency around 1 rad/s; (b) statistical description of sea states SSN4, 5, and 6. Higher sea state numbers correspond to more developed waves, for instance, generated along large distances, which have higher amplitudes and less frequency dispersion.*

surements are taken. The description column in Table 1 refers to terms like calm waters, rough sea, and very high waves, which are used by sailors to describe their subjective impression when exposed to the kind of waves given in Table 1.

Our research interest focuses on sea states (SS) N4, 5, and 6. Figure 1(b) shows the wave energy spectra for these three sea states.

Some towing tank facilities have a basin with a wavemaker for seakeeping studies. Using the wavemaker, it is possible to generate regular, periodic waves. In addition, sea states can be simulated by generating irregular, non-periodic waves, displaying statistical characteristics that are similar to those found in the sea [17].

Table 1. World Meteorological Organization sea states. Ten different sea states are specified in terms of wave height statistics and qualitative sea descriptions.

Sea State Code	Significant Wave Height Range (m)	Mean Significant Wave Height (m)	Description
0	0	0	Calm
1	0–0.1	0.05	Calm
2	0.1–0.5	0.3	Smooth
3	0.5–1.25	0.875	Slight
4	1.25–2.5	1.875	Moderate
5	2.5–4.0	3.25	Rough
6	4.0–6.0	5.0	Very rough
7	6.0–9.0	7.5	High
8	9.0–14.0	11.5	Very high
9	Over 14.0	Over 14.0	Phenomenal

A ship is a partially submerged body, with motion subject to hydrodynamic forces and moments [18]. The study of these forces and moments considers the effect of added mass due to the inertia of the surrounding water, damping caused by the water, restoring forces due to buoyancy and gravity, and the effects of incident waves. A set of simplified differential equations with coefficients that depend on sailing conditions, can be used to describe the dynamics of the ship. These equations have the form [17]

$$\begin{aligned}(m+a_{11})\ddot{x}_1 + b_{11}\dot{x}_1 &= (F_1 W)_{\gamma^1},\\ (m+a_{22})\ddot{x}_2 + b_{22}\dot{x}_2 + a_{24}\ddot{x}_4 + b_{24}\dot{x}_4 &\\ +a_{26}\ddot{x}_6 + b_{26}\dot{x}_6 + c_{26}x_6 &= (F_2 W)_{\gamma^2},\\ (m+a_{33})\ddot{x}_3 + b_{33}\dot{x}_3 + c_{33}x_3 &\\ +a_{35}\ddot{x}_5 + b_{35}\dot{x}_5 + c_{35}x_5 &= (F_3 W)_{\gamma^3} \qquad (2)\end{aligned}$$

$$\begin{aligned}a_{42}\ddot{x}_2 + b_{42}\dot{x}_2 + (I_{44}+a_{44})\ddot{x}_4 + b_{44}\dot{x}_4 &\\ +c_{44}x_4 + a_{46}\ddot{x}_6 + b_{46}\dot{x}_6 + c_{46}x_6 &= (F_4 W)_{\gamma^4},\\ a_{53}\ddot{x}_3 + b_{53}\dot{x}_3 + c_{53}x_3 &\\ +(I_{55}+a_{55})\ddot{x}_5 + b_{55}\dot{x}_5 + c_{55}x_5 &= (F_5 W)_{\gamma^5},\\ a_{62}\ddot{x}_2 + b_{62}\dot{x}_2 + a_{64}\ddot{x}_4 + b_{64}\dot{x}_4 &\\ +(I_{66}+a_{66})\ddot{x}_6 + b_{66}\dot{x}_6 + c_{66}x_6 &= (F_6 W)_{\gamma^6}, \qquad (3)\end{aligned}$$

where the subscripts are defined by: 1-surge, 2-sway, 3-heave, 4-roll, 5-pitch, 6-yaw. Furthermore,

- x_i are motion magnitudes
- m is the mass of the ship
- I_{ii} are the principal moments of inertia
- a_{ij} are the added masses
- b_{ij} are the damping coefficients
- c_{ij} are the restoring coefficients
- W is the input (waves)
- F_i and γ_i are the gain and phase of a function that transforms incident waves into forces and moments acting on the ship.

The left-hand side of the equations, which is the free response model of the system, relates forces and moments with linear movements and rotations. The right-hand side includes waves-to-forces and waves-to-moments relations, which comprise the forcing terms. The coefficients in the equations can be established from experiments with either real ships, scaled-down replicas, or computational fluid dynamics (CFD) programs.

With head seas, the vertical accelerations are related to pitching and heaving motions. As a result, this research focuses on (2) and (3). Notice that these two equations are not coupled with the rest of equations. With head seas, and when the distance between waves is short, the ship lies on two or more waves and the vertical motion is small. For long distances between waves, it is harder for the ship to lie on waves, and the vertical motion becomes large. Experiments show that there is a distance between waves, of the same order as the ship's length, that induces large vertical motions [19]–[23]. In seakeeping studies, results are frequently presented with RAOs, which are plots of output/input amplitude ratios obtained with sinusoidal approximation of the wave excitation and the resulting effects. Figure 2 displays RAOs of some experimental results involving pitching, heaving motion, and acceleration, where the horizontal axis denotes the wavelength of waves divided by the ship's length. The peak in Figure 2 occurs at the wavelength (frequency) denoted by **Lr** (ν**r**).

The wave frequency ω_o and wavelength λ_o are related by the equation

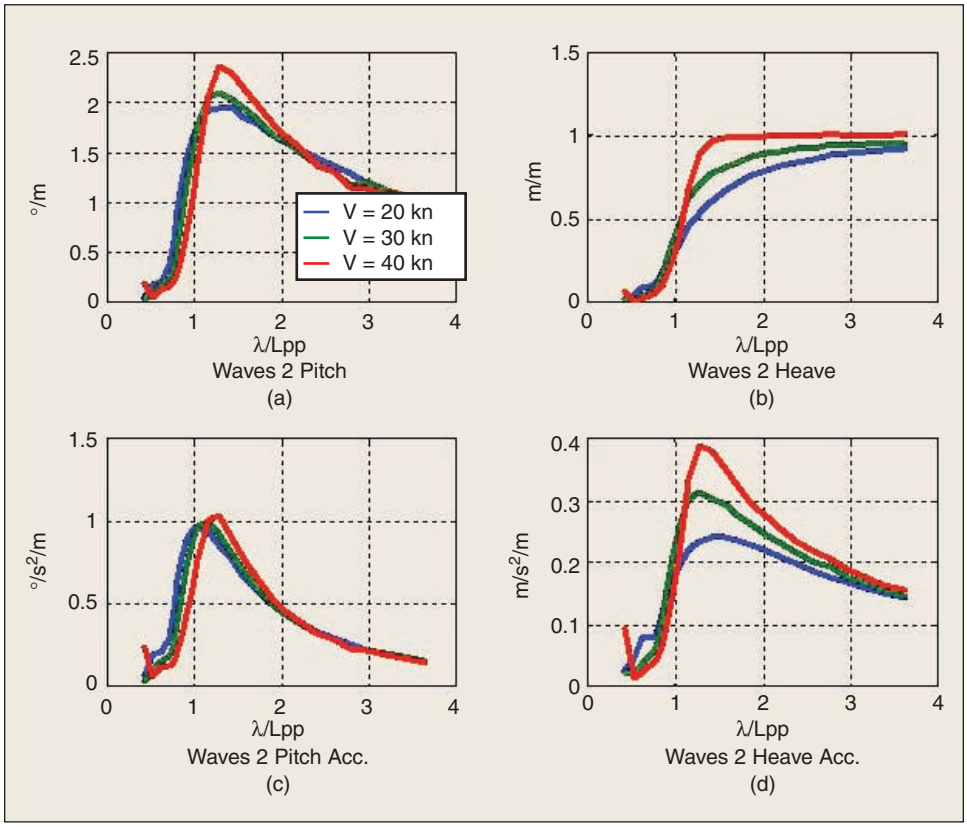

Figure 2. *RAOs of pitch and heave motions and accelerations: (a) pitch motion, (b) heave motion, (c) pitch acceleration, and (d) heave acceleration. The horizontal axes are wave wavelengths divided by the ship's length. Notice resonance peaks in the vertical accelerations when the excitation wavelength is close to the ship's length.*

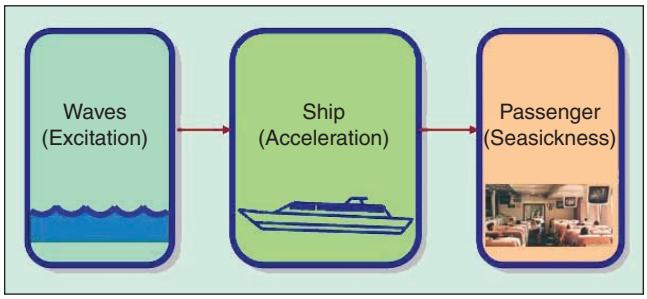

Figure 3. *Principal aspects (blocks) of the problem. The overall model can be seen as a chain of three filters. The ship is a bandpass filter, with a central frequency determined by the ship's length. Vertical oscillations induced by waves can cross the ship and seasickness filters, causing seasickness.*

$$\lambda_0 = \frac{2\pi g}{\omega_0^2}.$$

Suppose the ship is moving with speed U against head seas. The frequency of wave encounter is given by

$$\omega_e = \omega_o + \frac{\omega_o^2 U}{g}. \tag{4}$$

Since waves are approximately sinusoidal, it seems natural to follow a frequency domain approach for control based on the frequency of encounter. However, there are some special aspects to be considered.

- If there are regular waves with wavelength **Lr**, then the ship experiences large vertical motion corresponding to the gain peaks in Figure 2. The frequency of this motion obeys (4), and thus the frequency changes when the ship's speed U changes. Assuming that the gain peaks in Figure 2 are related to poles, these poles move as a function of U.
- The wave energy spectrum, as seen by the ship, shifts along the frequency axis according to U [17].
- The water surrounding the ship makes the dynamic characteristics of the ship depend on U, since added mass and damping are function of speed.

Figure 3 depicts the three main aspects of the problem. This diagram can be seen as a chain of three filters that may cause high MSI and depend on the ship's design (mainly its length), the sea state, and the ship's speed.

Research Steps

The ship considered in our research is the fast ferry shown in Figure 4. This ship, built by the Spanish shipbuilder company Izar, is 110 m long, can carry 1,250 passengers, has an aluminium deep-V monohull, and can reach 40 kn or more [24]–[26].

To reduce the vertical motion, there are two submerged actuators. Figure 5 shows the location of the actuators, which are dictated by the shipbuilder. The T-foil near the bow has two wings, which can rotate $\pm 15^\circ$ with respect to the horizontal. The two transom flaps can rotate between 0° and -15° with respect to the horizontal. There are hydraulic systems to move the actuators. These hydraulic systems are rate limited.

A relevant part of the experimental research has been accomplished with the help of Canal de Experiencias

Figure 4. *The high-speed ship. The vehicle is a 110-m-long, deep-V aluminium monohull ship, which carries 1,250 passengers at 40 kn. She uses waterjets and is operational in Europe and South America during the summer.*

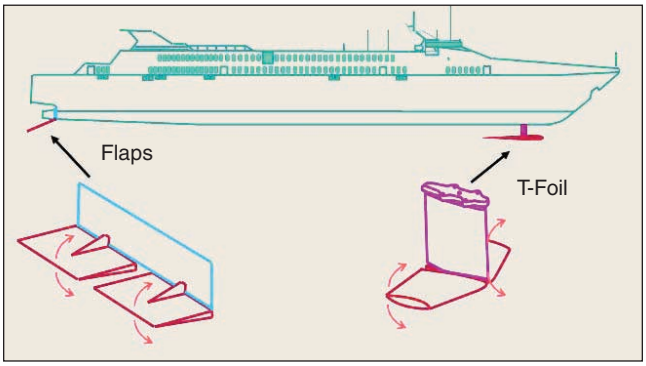

Figure 5. *Location of the actuators on the ship. The T-foil is near the bow, with fins that can rotate* $\pm 15^\circ$ *with respect to the horizontal. The transom flaps can rotate between* 0° *and* 15°. *The actuators are placed to maximize control moments with respect to vertical motion.*

Hidrodinamicas de El Pardo (CEHIPAR), Madrid [27]. This towing tank institution has a long channel to study drag forces, and a basin (150 m long × 30 m wide × 5 m depth) with a wavemaker. The tank has a computerized planar motion carriage in the basin, which can move like a large-scale plotter, with a scaled-down replica of the ship attached to it (Figure 6). With the help of a computerized system, many different kinds of waves can be generated. Thus, the behavior of the ship can be studied at different speeds and headings, under various sea conditions.

A 4.5-m 1/25 scaled-down replica of the fast ferry was built for modeling and control studies. This size exceeds the consensus among towing tank institutions that the minimum acceptable scale is 1/40. The main steps of the research were the following:

- Modeling of the pitching and heaving motion of the ship. The source data were provided by a CFD program. The validation data were experimental, using the scaled-down replica. These experimental data were obtained with regular waves (a set of 15 different wavelengths) and irregular waves corresponding to sea states SSN4, 5, and 6. The tests were done at replica speeds corresponding to ship speeds of 20, 30, and 40 kn.
- Modeling the actuators. Since information on actuators was scarce [28]–[31], a decision was made to design and implement custom devices. The physics-based calculations provided a mathematical model of the actuators' effects. Experiments were performed, using the replica with actuators to confirm the efficacy of the actuators and refine their mathematical models.
- Development of a simulation environment in SIMULINK to test control solutions. Confirmation experiments are meaningful only after the computer simulation is satisfactory.
- Establishing optimized control designs. The actuated ship is a complicated nonlinear system. Analytical approaches for control design are difficult. However, using a fast version of the simulation, any control structure can be tested and tuned. Since we already have experience in genetic algorithms (GA) as an alternative to search-based optimization, we combined GAs with fast simulation.
- Experimental confirmation of reference control designs. Satisfactory control solutions were obtained in simulation, and tested with the scaled-down replica.

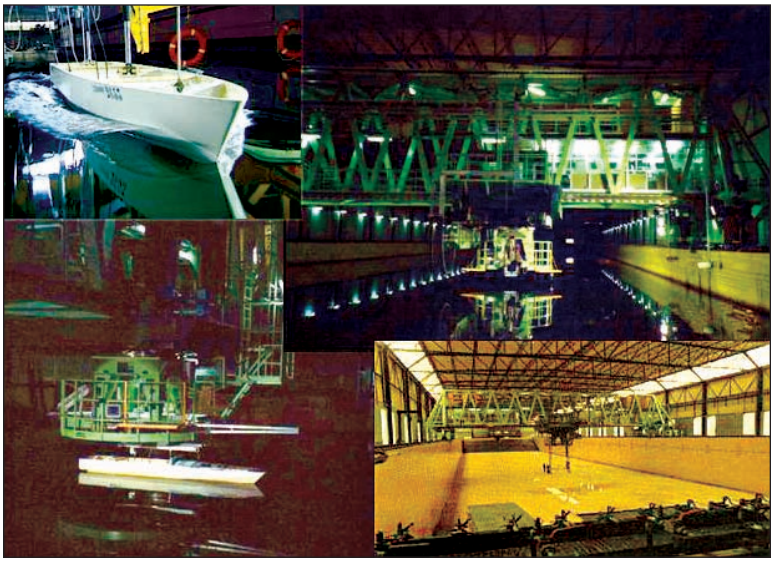

Figure 6. *Experimental devices and facility. Top left is the scaled-down replica on calm waters. Top right is a view of the 150 m* × *30 m basin with the wavemaker and computerized planar motion carriage. Bottom left is a detail of how the replica (4 m long) is attached to the carriage. Bottom right shows a view of the empty basin with people inside.*

Modeling the Vertical Ship Motions

Let us consider the ship without actuators. The models of the pitching and heaving motions of the ship are different for each speed. The model development departs from (2), and (3).

As a complementary tool, CEHIPAR uses a simulation program to predict the motion of a ship with regular sinusoidal waves. This CFD program is based on a CAD description of the hull and uses a finite element approach. The program gives the amplitudes and phases of the pitch and heave forces and motions, as well as the value of each coefficient in (2) and (3) for a set of wavelengths and ship's speeds. In this research we use 15 different wavelengths along with ship speeds of 20, 30, and 40 kn. Some coefficients a_{ij} and b_{ij} depend on the wavelength; see Figure 7.

Equations (2) and (3) can be combined to obtain a state equation of the system given by

$$\begin{bmatrix} \dot{x}_3 \\ \ddot{x}_3 \\ \dot{x}_5 \\ \ddot{x}_5 \end{bmatrix} = \begin{bmatrix} 0 & 1 & 0 & 0 \\ \frac{a_{35}c_{53}M_5 - c_{33}}{N_3} & \frac{a_{35}b_{53}M_5 - b_{33}}{N_3} & \frac{a_{35}c_{55}M_5 - c_{35}}{N_3} & \frac{a_{35}b_{55}M_5 - b_{35}}{N_3} \\ 0 & 0 & 0 & 1 \\ \frac{a_{53}c_{33}M_3 - c_{53}}{N_5} & \frac{a_{53}b_{33}M_3 - b_{53}}{N_5} & \frac{a_{53}c_{35}M_3 - c_{55}}{N_5} & \frac{a_{53}b_{35}M_3 - b_{55}}{N_5} \end{bmatrix} \times \begin{bmatrix} x_3 \\ \dot{x}_3 \\ x_5 \\ \dot{x}_5 \end{bmatrix} + \begin{bmatrix} 0 & 0 \\ \frac{1}{N_3} & -\frac{a_{35}M_5}{N_3} \\ -\frac{a_{55}M_3}{N_5} & \frac{1}{N_5} \end{bmatrix} \times \begin{bmatrix} (F_3W)_{\gamma^3} \\ (F_5W)_{\gamma^5} \end{bmatrix},$$

where

$$M_3 = 1/(m_{33} + a_{33}),\ N_3 = m_{33} + a_{33} - a_{35}a_{53}M_5,$$
$$M_5 = 1/(m_{55} + a_{55}),\ N_5 = m_{55} + a_{55} - a_{53}a_{35}M_3.$$

Model of Forces-to-Motions

Using the "ss2tf" MATLAB function, we obtain for each speed a set of four transfer functions relating forces and moments to motions. For instance, the transfer functions at 40 kn and the SSN4 predominant frequencies of encounter are given by

$$Fh2H(s) = \frac{0.000157(s^2 + 0.82s + 1.74)}{(s^2 + 0.6495s + 1.196)(s^2 + 0.9805s + 2.767)},$$
$$Mp2H(s) = \frac{0.00000166\,s(s + 0.21)}{(s^2 + 0.6495s + 1.196)(s^2 + 0.9805s + 2.767)},$$
$$Fh2P(s) = \frac{0.00000342\ (s + 0.22)}{(s^2 + 0.6495s + 1.196)(s^2 + 0.9805s + 2.767)},$$
$$Mp2P(s) = \frac{0.000000207\ (s^2 + 0.82s + 1.91)}{(s^2 + 0.6495s + 1.196)(s^2 + 0.9805s + 2.767)}.$$

Model of Waves-to-Forces

While the left-hand side of (2) and (3) offer an analytical basis for modeling forces-to-motions, the right-hand side of these equations does not model waves-to-forces. Fortunately, we can obtain data with the CFD program. For the three speeds, Figure 8 shows the source data given by the CFD program in the form of magnitude and phases of the wave-to-forces and wave-to-moments gains, versus frequency of wave encounter.

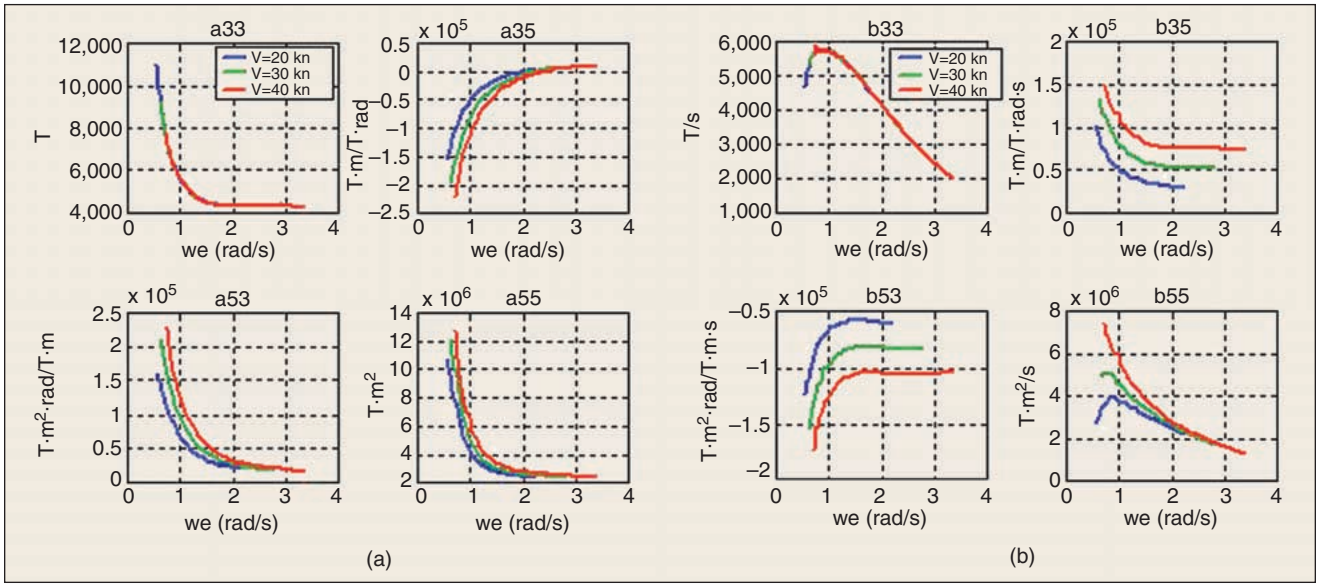

Figure 7. *Coefficients of (2) and (3). These coefficients depend on the frequency of encounter with waves and the ship speed: (a) added masses and (b) damping coefficients, at 20, 30, and 40 kn. The horizontal axes are frequencies of encounter in rad/s.*

To approach this aspect of the modeling, a method was developed as follows. First, we generate candidate transfer functions of different orders n and numerator order $m < n$, with coefficients to be determined. Second, we fit each candidate to the data curves by using GA to minimize the quadratic error of the curve fitting. The candidate that matches the data best is selected from those obtained with GA. We also refine the result by completing the procedure with local optimization. Consequently, the third step uses this best candidate as the initial value of a nonlinear least squares optimization with interval modeling. Using the method, the transfer functions of wave-to-forces and wave-to-moments are determined. The transfer functions for 40 kn are given by

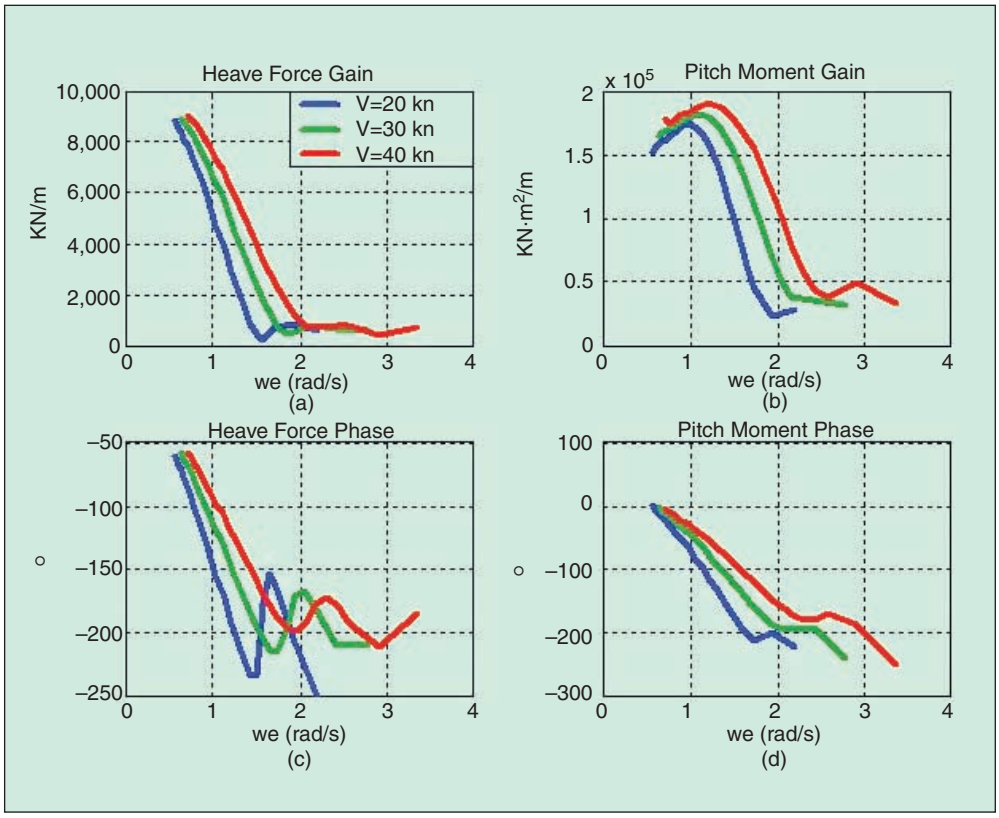

Figure 8. *Response of the forces and moments involved in the vertical motion of the ship at 20, 30, and 40 kn. This motion depends on the frequency of encounter with waves (rad/s): (a) magnitude of heave force, (b) magnitude of pitch moment, (c) phase of heave force, and (d) phase of pitch moment. Ordinates are linear. Notice how the ship speeds shift the responses. Recall that frequencies around 1 rad/s cause seasickness.*

$$W2Fh(s) = \frac{16450(s^2 - 0.468s + 5.128)(s^2 - 3.752s + 38.38)}{(s^2 + 3.043s + 2.907)(s^2 + 2.465s + 8.151)},$$

$$W2Mp(s) = \frac{76530(s - 5.711)(s - 0.5868)(s^2 - 0.4719s + 14.09)}{(s^2 + 3.015s + 3.557)(s^2 + 2.711s + 7.87)}.$$

The complete ship's model is described by the block diagram in Figure 9. Notice the cross-coupling between pitch and heave [32].

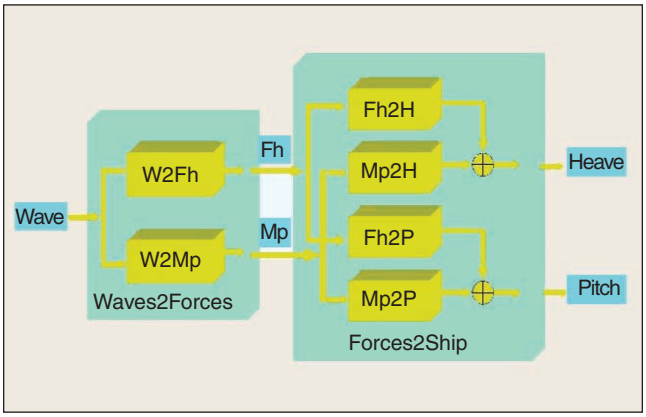

Figure 9. *Block diagram of the ship model. The blocks are transfer functions. The two blocks to the left are wave-to-forces models, while the four blocks to the right are forces-to-motions models. Notice the cross couplings.*

Experiments with regular waves were performed with the same 15 periods used by the CFD program. The magnitudes and phases of waves, heaving, and pitching motions were measured. A plot of these quantities versus the frequency of wave encounter can be used for a visual comparison with the model predictions. The validation was completed for the experiments with irregular waves. Figure 10 compares experimental and predicted heaving and pitching motions at 30 kn. Notice that the linear model agrees well with experimental data. There are only small differences near the peaks due to nonlinearities. The linear models for other speeds also show good agreement.

Notice that the control-oriented models have been

obtained based on a CAD description of the hull. This dependence is a useful advantage for control studies before a ship is built.

Modeling the Actuators

The design of the actuators was accomplished with the help of experts from CEHIPAR and Izar. The dimensions of the ship, the hydraulic cylinder capabilities, and the relevant physics dictate boundaries for the design. The T-foil wings are trapezoidal, with 3-m span, 2.5 maximum chord, 13.5 °/s maximum rotational speed, and ±15° maximum angle. The flaps are rectangular, with 4.8-m span, 1.1 chord, 13.5 °/s maximum rotational speed, and −15° maximum angle.

The actuators offer lift force, at the price of drag and other degrading phenomena, such as cavitation and turbulence. Sources of relevant information are [33]–[35]. The lift force is a function of the actuator angle α and the fluid speed U given by

$$F_L = \frac{1}{2}\rho A U^2 C_L(\alpha)\alpha,$$

where ρ is water density, A is actuator area, $C_L(\alpha)$ is lift coefficient, which for small α is nearly constant. The maximum effect of flaps on heave and pitch is summarized in Table 2. Compare these values with the effect of the waves computed with the ship models, as given in Table 3. At high speeds the actuators have more effectiveness. Calm waters, such as SSN4, cause smaller ship motions, heave forces, and pitch moments than rough sea conditions such as SSN6. Consequently, SSN4 and 40 kn provides the best combination of conditions for the significant use of the actuators to counteract wave-induced heave forces and pitch moments. Figure 11 shows the expected ideal heave and pitch acceleration drop with the actuators for 20, 30, and 40 kn, and SSN4. Both flaps and T-foil are used.

A complete SIMULINK model has been developed for the actuators [36]. The model detects the onset of cavitation, which occurs for certain combinations of pressure and fluid speed. The pitch angle of the ship is taken into account in calculating the effective angle of the wings.

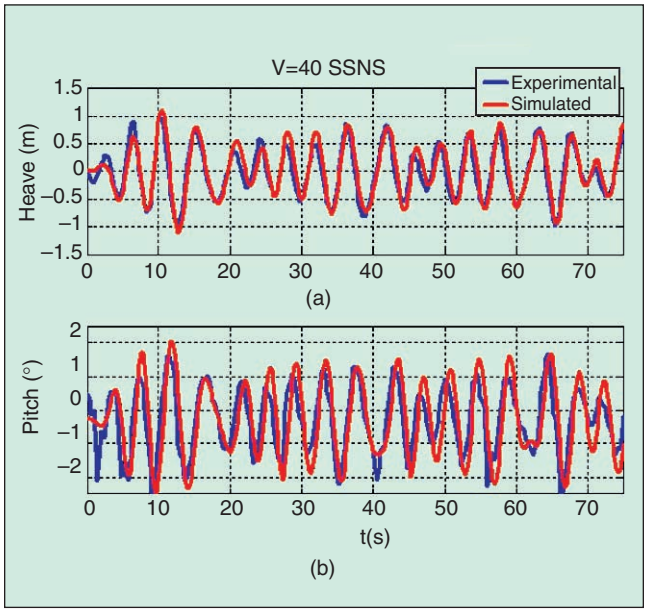

Figure 10. *Comparison of experimental and predicted (a) heave and (b) pitch motions. The phases agree well, while the differences at the peaks show the effect of nonlinearities. This figure shows part of a complete experimental data record along the basin, at 40 kn and SSN5.*

Table 2. The effect of the flaps on heave force and pitch moment increases in function of the ship's speed U.

U (kn)	$F_{\text{heave max.}}$ (kn)	$M_{\text{pitch max.}}$ (knm)
20	606	22,422
30	1,364	50,468
40	2,426	89,762

A Simulation Environment

The model of the ship's motion has two components. One component obtains forces and moments generated by the waves, while the other component obtains the heaving and pitching motions resulting from the forces and moments. An advantage of this approach is that the forces and moments obtained by the actuators can easily be coupled to the ship model. The complete system is multivariable, with two manipulated variables, the command signals for the flaps and the T-foil. The waves are a perturbation to the system. The ship and actuator models have been developed to be easily coupled, as shown in Figure 12. By adding to this nucleus a source of excitations (regular or irregular waves), sensor models (to consider bandwidth and noise), and control of the actuators, we obtain a complete model of the controlled system in its operational environment. By adding display and data input interfaces to the complete model, we obtain a useful tool for control design purposes. A simulation environment was implemented.

Figure 13 shows a computer screen of the simulation environment [37], [38]. The user can open several windows to observe a simulated journey. For instance, the windows in a horizontal row at the top of the screen show the T-foil movement and plot the vertical acceleration at the worst place (WVA). Other windows can be opened to study pitching and heaving motions or accelerations, and to see the waves. The user can select regular waves with 15 different periods or irregular waves (SSN4, 5, or 6), and the ship's speed (20, 30, or 40 kn). There are two larger windows at the bottom of Figure 13. One contains the complete model, with the controller block being editable. The other window shows the ship moving. The top of this window displays

the motion of the flaps and the T-foil, and the increase in MSI as represented by an increasing horizontal bar.

Some preliminary experiments were done with conventional proportional-integral derivative (PID). There was a lot of noise from sensors, which was amplified by derivative action. Based on spectral analysis of signals and noise, a digital filter was designed to reject noise and bias, while minimizing phase modification in the frequency range of the control. To make the simulation environment more realistic, the experimental sensor noise was recorded and included in the models.

Studies on seasickness published in 1974 conclude that seasickness is a cumulative effect related to vertical acceleration at certain frequencies.

The simulation is suitable for testing different controller specifications, for instance, by systematically changing PID parameters. This tuning should be done quickly and automatically. Consequently, a fast version of the simulation was also developed and a batch mode was provided. A set of quality indexes was defined, including the final MSI, the number of reversing motions of the actuators, the time intervals of cavitation, and the number of keel slams. The batch procedure gives a final table with indexes to help compare control results for different control specifications.

Control Design Studies

Once the simulation environment was ready, the research considered several control alternatives. A good control target is to minimize the MSI. Several types of sensors can be employed for the feedback control implementation. For instance, an accelerometer that measures WVA in the ship, or an inertial unit for the on line measurement of pitch and heave. Thinking in practical terms, it is clear that PID controllers should be the first candidates to be

Table 3. The wave-induced heave forces and pitch moments acting on the ship increase in function of the sea state number (SSN) and the ship's speed (U).

SSN	U (kn)	$F_{heave\ max.}$ (kn)	$M_{pitch\ max.}$ (knm)
4	20	3,389	221,280
5	20	6,779	387,230
6	20	10,169	497,870
4	30	6,101	276,600
5	30	13,558	442,550
6	30	18,981	663,830
4	40	8,134	309,790
5	40	16,848	553,190
6	40	23,727	774,470

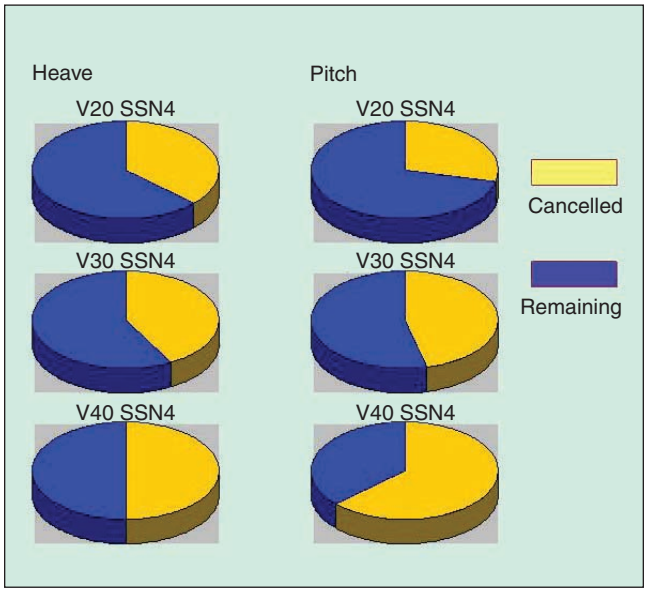

Figure 11. *Expected and ideal heave and pitch acceleration reduction with actuators. Higher speeds allow for better actuator effectiveness.*

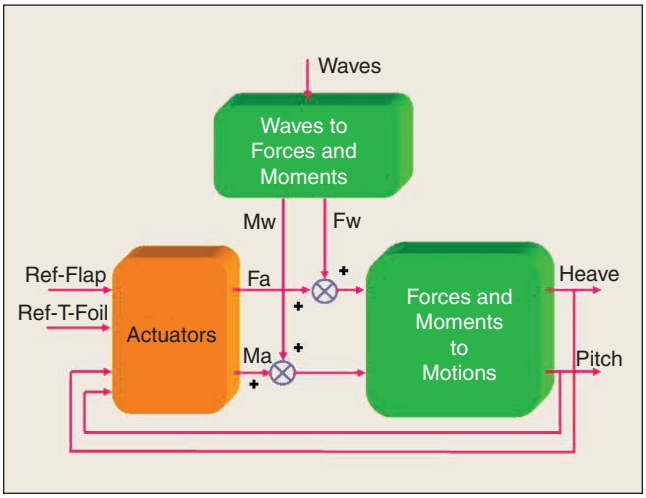

Figure 12. *Diagram of the ship-actuator system. The actuators must counteract the forces and moments induced by incident waves. Notice how the structure of the ship model (Figure 9) is well suited to include the actuators with an easy connection of blocks. Heave and pitch are fed back to the actuators.*

tested as a reference for further improvements. Preliminary PID control experiments showed that integral action has detrimental effects; therefore PD control was selected. As discussed below, two PD control versions were studied in the simulation environment.

Using an Accelerometer

Taking the MSI as the principal quality measure to be minimized, a systematic exploration of parameters of two PD controllers (one for the flaps, the other for the T-foil) was performed using the simulation [39]. Both PDs use an accelerometer measuring the WVA. Figure 14(a) shows a three-dimensional view of flap response, and Figure 14(b) shows the T-foil response. A complete set of Kd and Kp values was tested, and the results are displayed in the figure. Optimal tunings for the three speeds were obtained. Using the simulation as a fitting function, GA was used to find the optimal PD or general controller tuning.

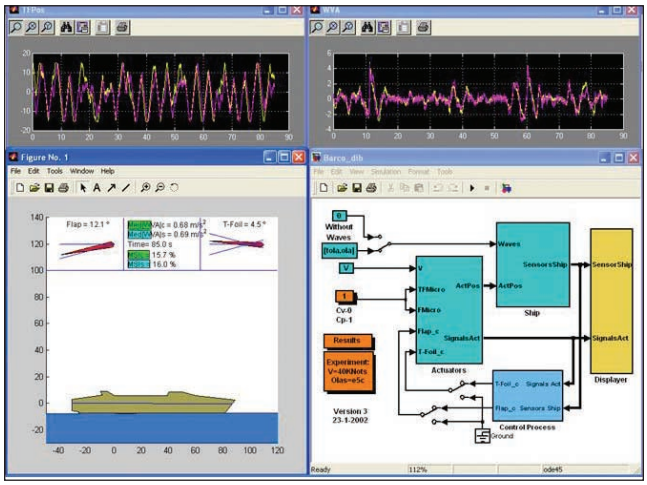

Figure 13. *Main screen of the simulation environment in SIMULINK. There is a window with the SIMULINK diagram of the blocks supporting the simulation; the user can edit the controller block to study various control strategies. Another window, using animated graphics, shows the motion of the ship and the actuators, as well as the increase of the MSI along the simulated journey. Other windows can be opened to show the time record of the signals of interest.*

Using an Inertial Unit

The multi-input/multi-output (MIMO) approach, based on measurements of pitch and heave, was applied using a multivariable PD controller [40]; see Figure 15. Bidirectional flap action is obtained by trimming them at -7.5° when the command signal is zero, and moving the flaps within the range 0° to -15° (that is $+7.5^\circ$ around the middle value) otherwise.

The block W (Figure 15) is an uncoupled filter

$$W = \begin{bmatrix} w_{11} & w_{12} \\ w_{21} & w_{22} \end{bmatrix} = \begin{bmatrix} 1 & \frac{-G_{12}}{G_{11}} \\ \frac{-G_{21}}{G_{22}} & 1 \end{bmatrix},$$

the transfer functions G_{C1} and G_{C2} are given by

$$G_{C1} = K_{P1}\left[\frac{1 + 1.1T_{D1}s}{0.1\,T_{D1}s + 1}\right], \quad G_{C2} = K_{P2}\left[\frac{1 + 1.1T_{D2}s}{0.1\,T_{D2}s + 1}\right],$$

and the parameters vector θ is defined by

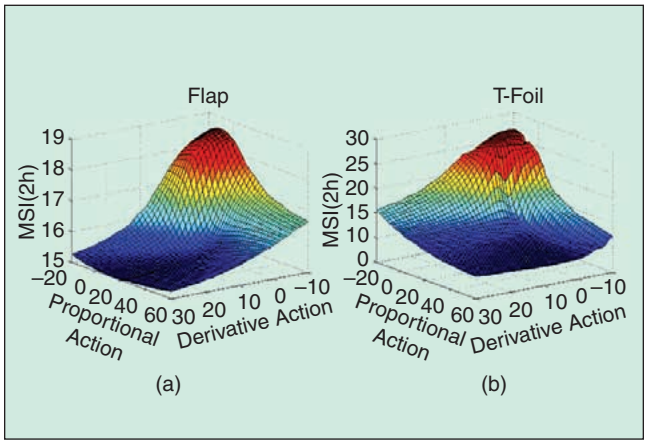

Figure 14. *Parameters of a PD controller have been systematically studied for tuning purposes: (a) PD tuning to minimize the MSI with the flaps and (b) PD tuning to minimize the MSI with the T-foil. Peaks indicate undesirable behavior, while valleys are desirable. Slightly different optimal tunings are obtained in the two three-dimensional plots.*

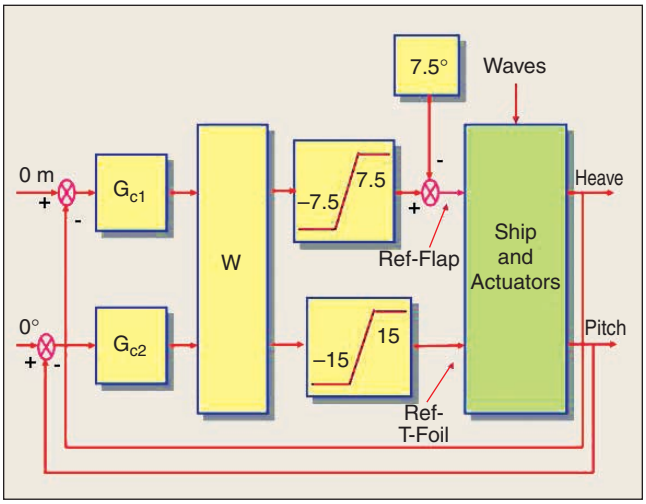

Figure 15. *Diagram of MIMO control. The ship-actuators block is detailed in Figure 12. A flap trim angle of 7.5° is imposed, to obtain variations of ±7.5° around this angle (that is, rotations between 0° and 15°).*

$$\theta = [K_{P1}, T_{D1}, K_{P2}, T_{D2}]^T.$$

Tuning of the controllers G_{C1} and G_{C2} is done by solving a nonlinear optimization problem

$$J(\theta_{\text{opt}}) = \min_{\theta \in S} J,$$

where J is the MSI and S is the set of allowed values of the parameters in θ. These ranges have been established according to the following criteria: G_{C1} and G_{C2} must be stable, long saturation states of the actuators must be avoided, and frequencies in the range $\omega_e = [0.1, 10]$ rad/seg must be considered, where the waves energy excites the process.

In simulation, this control strategy does not improve the MSI with respect to the dual PD, although it is an interesting basis for further studies.

Experimental Results

Control experiments require completing the model with actuators, sensors, and a digital processing system. Figure 16 shows the model out of the water, with the flaps and T-foil, during the assembly process. Five accelerometers were installed along the hull, one of which was located near the bow, where passenger vertical acceleration is maximized (WVA). Additional devices measure pitching and heaving motions.

An industrial PC with a 200 MHz Pentium is in charge of the control. The PC is equipped with data acquisition subsystems for the sensors, and interface electronics to move the actuators. By using EdROOM, an automatic real-time control code generation tool developed by our group [41], experimental testing of control strategies can be performed easily and quickly. Experiments frequently

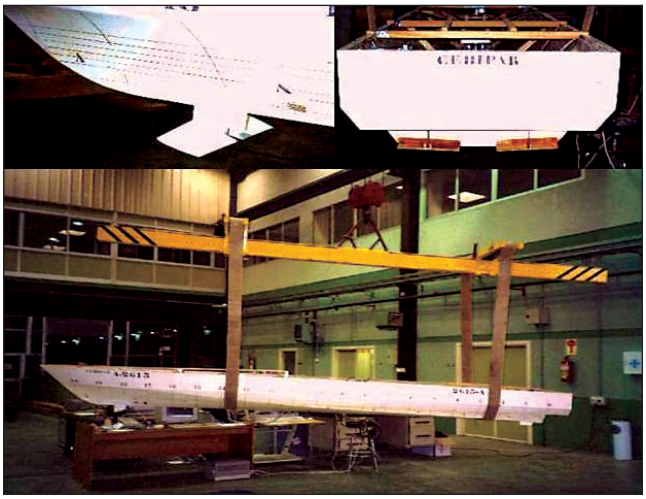

Figure 16. *The scale model out of the water. At bottom, the scale model is hanging from a fulcrum attached to a crane, which allows verification of actuator motion. Top left is a view of the T-foil, while top right is the transom flaps. The actuators are moved by electric motors.*

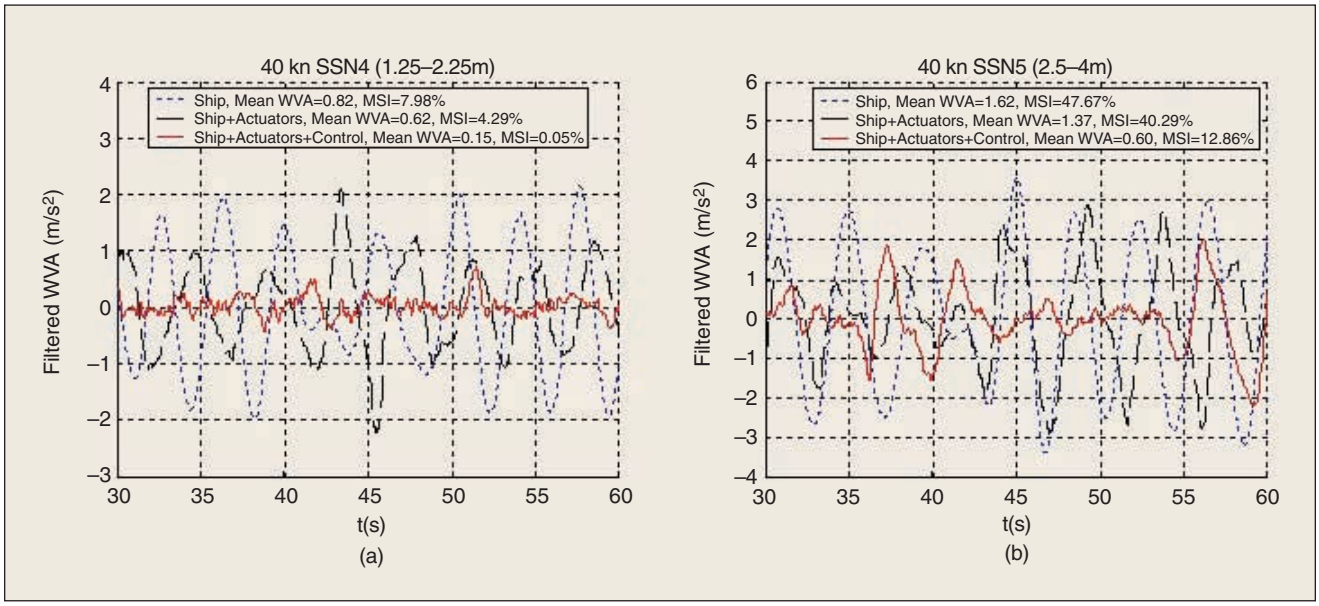

Figure 17. *Experimental results with irregular waves at 40 kn. The plots compare the WVA without actuators, with fixed actuators, and with controlled moving actuators. In (a) the WVA is shown with sea state SSN4; without actuators the MSI is 7.98%, with fixed actuators it is 4.29%, and with controlled moving actuators it is 0.05%. In (b) the WVA is shown with SSN5; the MSI is 47.67% without actuators, 40.29% with fixed actuators and 12.86% with controlled moving actuators. Recall that the MSI is the percent of passengers who get sick after two journey hours. The normal operation of the ship is with SSN4 or less.*

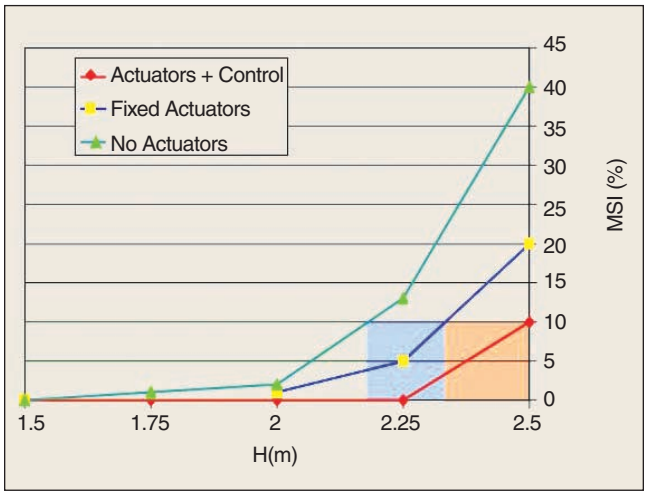

Figure 18. *The ship's operational range is expanded. The plot shows the MSI as a function of the wave height, for the ship without actuators, with fixed actuators, and with controlled moving actuators. Suppose the captain decides to sail if the expected MSI is less than 10%. It is clear from the figure that, with control and moving actuators, the ship can tolerate heavier sea conditions. Notice also that the region with 0% MSI is larger with controlled moving actuators.*

prompt improvements or modifications, which are facilitated by EdROOM.

A complete series of control experiments were performed using WVA measurement and the optimal dual PD control determined by the simulation. All combinations of ship's speeds (20, 30, and 40 kn) and sea states SSN4, SSN5, and SSN6 were studied with several basin runs per case. A complete run is equivalent to real ship motion along 3 km. The recorded data confirmed that the mean variables of interest converged to stationary values before the run was completed. The results presented in Figure 17(a) and (b) focus on a small part of one experiment. We comment on the results obtained for the most common cases during the ship's operation: 40 kn and SSN4, 40 kn and SSN5.

Figure 17(a) shows the experimental results at 40 kn with SSN4. The ordinates are mean WVA. There are three curves. One curve, with large variance, corresponds to the ship without actuators (MSI = 7.98%). Another, with medium variance, corresponds to the ship with fixed actuators (MSI = 4.29%). The last curve, with small variations, corresponds to the ship with actuators and optimal PD control (MSI = 0.05%). Figure 17(b) shows the experimental results at 40 kn and SSN5. Without actuators, the MSI is 47.67%. With fixed actuators, the MSI is 40.29%. With actuators and optimal PD control, the MSI is 12.86%.

Crossings could be canceled if it were thought that many people could become seasick, causing a negative economic impact. We assume that the limit enforced by the captain is MSI = 10%. Figure 18 depicts the MSI as a function of the wave height, without actuators, with fixed actuators, and with moving controlled actuators, at 40 kn. This figure shows that, by using actuators and control, the ship can tolerate higher waves, increasing the operational range of the ship. Notice also that the range with 0% MSI is extended.

Conclusions

This article describes research on ship vertical motion smoothing, using controlled flaps and a T-foil. SIMULINK models and a simulation environment were developed to facilitate control studies. Every step was carried out on an experimental basis.

The type of sensors used in the research, accelerometers or inertial units, can easily be introduced in real ships. The type and physical characteristics of the actuators we use have been determined by naval engineers, and are in active use in several ships.

Since the actuators have limited action (insufficient forces and moments, compared to the effects of waves), there is a limited margin for improvement based on more sophisticated control strategies. Possible improvements of MSI are linked to a control strategy that exploits better synchronization with incident waves.

During the experiments the control caused cavitation problems and excessive motion reversing of the actuators (excessive gain). Currently, the point of view regarding optimization has changed. It is interesting to trade a little MSI for better performance of the actuators. A logical consequence seems to be a multiobjective treatment of the control problem. The present aim of our research is to obtain satisfactory results on several fronts: good MSI, slamming suppression, less cavitation, and less motion reversing.

Several groups are now involved in the research, and various control alternatives are under study, including multiobjective optimization, QFT, and fuzzy control. A Web site [42] is available for coordination purposes. The site contains experimental and theoretical information, results of different control strategies, and videos of the experiments.

Acknowledgments

The authors want to thank the support of the MCYT Spanish Ministry (projects TAP970607-C03-01 and DPI2000-0386-C03-02) and the collaboration of the Izar and the CEHIPAR staff.

References

[1] C. Kennell, "Design trends in high-speed transport," *Marine Tech.*, vol. 35, no. 3, pp. 127–134, 1998.

[2] M.A. Abkowitz, "The effect of antipitching fins on ship motion," *SNAME Trans.*, vol. 67, pp. 210–252, 1959.

[3] G.P. Stefun, "Model experiments with fixed bow antipitching fins," *J. Ship Research*, vol. 3, no. 2, pp. 15–23, 1959.

[4] E.V. Lewis, "Increasing the sea speed of merchant ships," *SNAME Trans.*, vol. 67, pp. 757–772, 1959.

[5] K.M. Ochi, "Hydroelastic study of a ship equipped with an antipitching fin," *SNAME Trans.*, vol. 69, pp. 281–337, 1961.

[6] J.H. Vugts, "Pitch and heave with fixed and controlled bow fins," *Int. Shipbuilding Progress*, vol. 15, no. 3, pp. 191–215, 1967.

[7] M. Besso and Y. Kyozuka, "On the ship motion reduction by antipitching fins in head seas," in *Proc. 15 Symp. Naval Hydrodynamics*, 1984, pp. 109–118.

[8] J. Avis, "Use of antipitch foil to reduce added resistance of a yatch in waves," *Marine Tech.*, vol. 28, no. 1, pp. 15–22, 1991.

[9] M. Ryle, "Smoothing out the ride," *The Motor Ship*, pp. 23–26, Jan. 1998.

[10] A.J. Duncan, A.J. Haywood, and K.P. Klaka, "Ride control system (final report)," Rep. AMECRC-93-CP3, Curtin Univ., Perth, Australia, 1993.

[11] A.J. Haywood, A.J. Duncan, and K.P. Klaka, "The development of a ride control system for a surface effect ship. Interim report," Rep. CMST-C94-9, Curtin Univ., Perth, Australia, 1994.

[12] A.J. Haywood, A.J. Duncan, K.P. Klaka, and J. Bennett, "The use of simulation in the development of a ride control system for fast ferries," in *Proc. Conf. Maneuvering and Control of Marine Craft*, 1994, pp. 261–269.

[13] A.J. Haywood, A.J. Duncan, K.P. Klaka, and J. Bennet, "The development of a ride control system for fast ferries," *Contr. Eng. Practice*, vol. 3, no. 5, pp. 695–703, 1995.

[14] A.J. Haywood and A.J. Duncan, "Experiences using system identification techniques on high speed ferries," in *Proc. FAST'97*, 1997.

[15] C.R. Swanton, A.J. Haywood, and B.H. Schaub, "Simulation—An essential tool in the design of motion control systems," in *Proc. FAST'99*, 1999, pp. 73–81.

[16] J.F. O'Hanlon and M.E. MacCawley, "Motion sickness incidence as a function of frequency and acceleration of vertical sinusoidal motion," *Aerospace Med.*, Apr. 1974.

[17] A.R.J.M. Lloyd, *Seakeeping: Ship Behavior in Rough Weather*. Hampshire, U.K.: A.R.J.M. Lloyd, 1998.

[18] T.J. Fossen, *Guidance and Control of Ocean Vehicles*. New York: Wiley, 1994.

[19] B.V. Korvin-Kroukovski, "Investigation of ship motions in regular waves," *SNAME Trans.*, vol. 63, pp. 386–435, 1955.

[20] B.V. Korvin-Kroukovski and W.R. Jacobs, "Pitching and heaving motions of a ship in regular waves," *SNAME Trans.*, vol. 65, pp. 590–632, 1957.

[21] J.A. Ewing and G.J. Goodrich, "The influence of ship motions of different wave spectra and the ship length," *Trans. RINA*, vol. 109, pp. 47–63, 1967.

[22] N. Salvesen, E.O. Tuck, and O. Faltinsen, "Ship motions and sea loads," *SNAME Trans.*, vol. 78, pp. 250–285, 1970.

[23] N. Fonseca and C. Guedes Soares, "Time-domain analysis of large-amplitude vertical ship motions and wave loads," *J. Ship Res.*, vol. 42, no. 2, pp. 139–153, June 1998.

[24] A. Moret, A. Perez de Lucas, and J.L. Tejedor, "Fast ferry Mestral: A reliable answer in fast ferry design," in *Proc. FAST'93*, 1993, pp. 1269–1282.

[25] Anonymous, "126 m long Spanish fast ferry launched," *Fast Ferries*, pp. 19–20, Sept. 1996.

[26] Anonymous, "Silvia Ana: Results of first year`s service," *Ship&Boat Intl.*, pp. 15–16, Jan./Feb. 1998.

[27] CEHIPAR [Online]. Available: www.cehipar.es

[28] P. Mandel, "Some hydrodynamic aspects of appendage design," *SNAME Trans.*, vol. 61, pp. 464–515, 1953.

[29] W.L. Cave and D.S. Cusanelli, "Effect of stern flaps on powering performance of the FFG-7 class," *Marine Tech.*, vol. 30, no. 1, pp. 39–50, 1993.

[30] D.S. Cusanelli and L. Hundley, "Stern flap powering performance on a Spruance class destroyer," *Naval Eng. J.*, vol. 111, no. 1, pp. 69–81, Mar. 1999.

[31] M.R. Cocklin, M.G. Parsons, and A.W. Troesch, "Stern flap performance prediction for the coast guard 110-Foot WPB Island class patrol boat," *Marine Tech.*, vol. 37, no. 2, pp. 100–110, 2000.

[32] T. Havelock, "The coupling of heave and pitch due to speed of advance," *Trans. INA*, vol. 98, pp. 246–251, 1955.

[33] E.V. Lewis, *Principles of Naval Architecture*, Society of Naval Architects & Marine Engineers (SNAME), New Jersey, 1989.

[34] T. Kawazoe, S. Nishikido, and Y. Wada, "Effect of fin area and control methods on reduction of roll motion with fin stabilizers," *Bull. M.E.S.J.*, vol. 22, no. 1, pp. 25–32, Mar. 1994.

[35] R.P. Dallinga, "Hydrodynamical aspects of the design of fin stabilizers," *Trans. RINA*, pp. 189–200, 1993.

[36] S. Esteban, J.M. De la Cruz, J.M. Giron-Sierra, B. De Andres, J.M. Diaz, and J. Aranda, "Fast ferry vertical acceleration reduction with active flaps and T-foil," in *Proc. IFAC Intl. Symp. Maneuvering and Control of Marine Craft MCMC 2000*, Aalborg, Denmark, 2000, pp. 233–238.

[37] S. Esteban, J.M. Giron-Sierra, J.M. De la Cruz, and B. De Andres Toro, "A computer based testbed for designing the control of vertical motions of a fast ferry," in *Proc. Int. Conf. Marine Simulation and Ship Maneuvering, MARSIM 2000*, Orlando, FL, 2000, pp. 79–83.

[38] S. Esteban, B. De Andres, J.M. Giron-Sierra, O.R. Polo, and E. Moyano, "A simulation tool for a fast ferry control design," in *Proc. IFAC Intl. Conf. Control Applications in Marine Systems CAMS 2001*, Glasgow, U.K., 2001.

[39] J.M. Giron-Sierra, S. Esteban, B. De Andres, J.M. Diaz, and J.M. Riola, "Experimental study of controlled flaps and T-foil for comfort improvement of a fast ferry," in *Proc. IFAC Intl. Conf. Control Applications in Marine Systems CAMS 2001*, Glasgow, U.K., 2001.

[40] J. Aranda, J.M. Diaz, P. Ruiperez, T.M. Rueda, and E. Lopez, "Decreasing of the motion sickness incidence by a multivariable classic control for a high speed ferry," in *Proc. IFAC Intl. Conf. Control Applications in Marine Systems CAMS 2001*, Glasgow, U.K., 2001.

[41] O.R. Polo, S. Esteban, A. Maron, L. Grau, and J.M. De la Cruz, "Control code generator used for control experiments in ship scale model,"

in *Proc. IFAC Intl. Conf. Control Applications in Marine Systems CAMS 2001*, Glasgow, U.K., 2001.

[42] CRIBAV Web site: ctb.dia.uned.es/CRIBAV/

Jesus M. De la Cruz received the Licentiate (1979) and the Ph.D. (1984) degrees in physics from the Universidad Complutense de Madrid, Spain. In 1986 he joined the Open University of Spain, and in 1990 he became a full professor in the Universidad de Cantabria. In 1992 he joined the Department of Computer Architecture and Automatic Control at the Universidad Complutense de Madrid. He is the author of over 90 publications. His research covers several topics of applied automatic control and simulation: ships, airplanes, spacecrafts, robotics, logistics, and process control. His research interests currently focus on control system design, system identification, optimization, and simulation.

Joaquín Aranda received the Licentiate degree from the University Complutense of Madrid in 1983 and the Ph.D. degree from the Universidad Nacional de Educación a Distancia (UNED) in 1989. He was a teaching assistant in the Department of Computer Science and Automatic Control, University Complutense of Madrid, and an assistant professor, associate professor, and senior professor at the UNED. He was deputy director of the Computer Science University School of UNED and director of Computer Science High School. He is author or coauthor of over 70 publications. His scientific activities within the control engineering field include robust control, computer control, modeling and simulation of continuous processes, and application of control and simulation to high speed craft, airplane and robotic.

Jose M. Giron-Sierra (gironsi@dacya.ucm.es) received the Licentiate (1972) and the Ph.D. (1978) degrees in physics from the Universidad Complutense de Madrid, Spain. Since 1988 has been a senior professor with the Department of Computer Architecture and Automatic Control of the Universidad Complutense de Madrid, Spain. He is the author or coauthor of over 80 publications. He holds two patents for a robot and a communication system. His research is related to applied automatic control and simulation: ships, airplanes and spacecrafts, robotics, logistics, and process control. His research interests are high-speed ships, simulation, real-time remote monitoring and control, optimization based on genetic algorithms, and estimation with neural networks. He is a member of the IFAC Technical Committee on Marine Systems; he belongs to IEEE, AIAA, and EUROSIM. He can be contacted at the Dept. Arquitectura de Computadores y Automática, Universidad Complutense de Madrid. Ciudad Universitaria, 28040 Madrid, Spain.

Francisco Velasco received the Licentiate degree from the University of Santander in 1980 and the Ph.D. degree from the Universidad Nacional de Educación a Distancia (UNED) in 1993. He was a teaching assistant, associate professor, and senior professor in the School of Civil Marine of Santander, and as senior professor at the University of Cantabria. He is author or coauthor of over 50 publications. His scientific activities are in the field of control engineering, with focus on marine craft control. He is working in several research projects on this topic, taking advantage of the marine facilities at Santander harbor.

Segundo Esteban received the Licentiate (1996) and the Ph.D. (2002) degrees in physics from the Universidad Complutense de Madrid, Spain. He has been an assistant professor with the Department of Computer Architecture and Automatic Control of the Universidad Complutense de Madrid, Spain, since 1997. He is author or coauthor of 20 publications. He is involved in research on control of high-speed ships, simulation, and cooperative behaviors.

Jose M. Diaz received the Licentiate (1996) and the Ph.D. (2002) degrees in physics from the Universidad Nacional de Educación a Distancia (UNED) in 2002. He is teaching assistant in the Department of Computer Science and Automatic Control, UNED. He is author or coauthor of more than 20 publications. He is active in research on control of high-speed ships and robust control.

Bonifacio de Andres-Toro received the Licentiate (1977) and the Ph.D. (1996) degrees in physics from the Universidad Complutense de Madrid, Spain. He has been a senior professor with the Department of Computer Architecture and Automatic Control of the Universidad Complutense de Madrid, Spain, since 2002. He is author or coauthor of 60 publications. His research is related to applied automatic control and simulation for ships, logistics, and process control. His research interests include high-speed ships, simulation, and optimization based on genetic algorithms.